

# Indirect 3D-Space Vector Modulation for a Matrix Converter

Ahmed Abdelrehim

Department of Electrical Engineering  
Alexandria University  
Alexandria, Egypt  
ahmed.abdelrehim@siemens.com

Mohamed El-Habrouk

Department of Electrical Engineering  
Alexandria University  
Alexandria, Egypt  
eepgmmel@yahoo.com

Samir Deghedie Erfan

Department of Electrical Engineering  
Alexandria University  
Alexandria, Egypt  
deghedie@gmail.com

Karim Hassan Youssef

Department of Electrical Engineering  
Alexandria University  
Alexandria, Egypt  
khmyoussef@yahoo.com

**Abstract**—This paper discusses the indirect space vector modulation for a four-leg matrix converter. The four-leg matrix converter has been proven to be a reliable, cost-effective, and compact power electronic interface to supply unbalanced or nonlinear loads. However, the added fourth leg has shifted the inverter side modulation from simple two-dimension SVM into complex three-dimension. This paper employs a new technique to implement indirect 3D SVM in digital controllers with further simplification in the modulation process. Moreover, Simulink simulation using repetitive controller has been performed to regulate the output voltage for 400 Hz Power supplies.

**Keywords**—repetitive controller; 3D SVM; four-leg matrix converter

## I. INTRODUCTION

The matrix converter is a static and direct AC to AC converter with unique features of unity input power factor, high power to volume ratio, high reliability and MTBF factor which has gained interest in applications aiming to produce a realization of a compact three-phase drive for military, industrial and aerospace systems [1-3]. Moreover, researchers utilized the matrix converter as an electronic interface layer between all resources (wind, solar, storage, etc.) of the energy matrix model and as an electronic transformer competing with the traditional magnetic transformer. The added fourth leg is placed to provide a return path for the zero-sequence current during unbalancing and add the capability of supplying different connected single-phase loads. Four-leg converters have a superior ability to produce balanced output voltage waveform even under severely unbalanced load or non-linear load conditions [4]. A four-leg matrix converter topology is shown in Figure 1. This paper investigates the indirect space vector modulation which decouples the modulation into two stages (rectifier + inverter) without intermediate energy storage. This decoupling is efficient and allows separate control

to each stage, while as there is no intermediate energy storage, a proper synchronization between the two stages is mandatory to fulfill the power balance equation as instantaneous input power shall be equal to the instantaneous output power for the load [5]. At high-frequency applications with precise control requirements as for naval and aerospace applications where the 115V-400Hz system is commonly used, traditional controllers have failed to achieve a proper regulation, due to the limited bandwidth so the repetitive controller is introduced as an optimum solution for this control problem [6].

## II. MATRIX CONVERTER MODEL

Matrix converter can be represented mathematically by matrix  $M$  and switches are identified as  $S_{xy}$ , where  $X$  is the output phase,  $Y$  is the input phase and  $S$  is the linking switch between input and output. Rectifier switches are numbered from  $S_1$  to  $S_6$  while inverter side switches are numbered from  $S_7$  to  $S_{14}$ . The rectifier is represented in Figure 1. Governing equations are:

$$V_{out} = M * V_{in} \quad (1)$$

$$I_{out} = M^T * I_{in} \quad (2)$$

$$V_{out} = M_i * V_{DC} \quad (3)$$

$$V_{DC} = M_R * V_{in} \quad (4)$$

$$V_{out} = M_i * M_R * V_{in} \quad (5)$$

where  $V_{out}$ ,  $V_{in}$ ,  $I_{out}$ ,  $I_{in}$ ,  $V_{DC}$ ,  $M_i$ ,  $M_R$ ,  $M$  and  $M^T$  are output voltage, input voltage, output current, input current, DC intermediate voltage, inverter side switching matrix, rectifier side switching matrix, matrix converter switching matrix and transposed matrix converter switching matrix respectively.  $M_R$  and  $M_i$  are described by (6) and (7) respectively:

$$M_R = \begin{bmatrix} S_1 & S_3 & S_5 \\ S_2 & S_4 & S_6 \end{bmatrix} \quad (6)$$

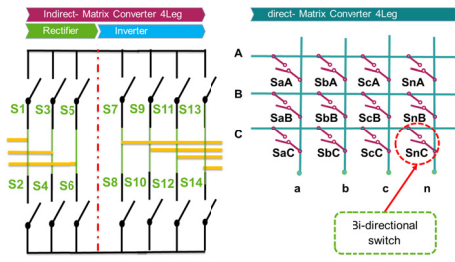


Fig. 1. Schematic of a four-leg direct matrix converter

$$M_i = \begin{bmatrix} S7 & S8 \\ S9 & S10 \\ S11 & S12 \\ S13 & S14 \end{bmatrix} \quad (7)$$

M equals to  $M_i * M_R$ :

$$M = \begin{bmatrix} S7 & S8 \\ S9 & S10 \\ S11 & S12 \\ S13 & S14 \end{bmatrix} * \begin{bmatrix} S1 & S3 & S5 \\ S2 & S4 & S6 \end{bmatrix} \quad (8)$$

Equation (8) can be further synthesized into

$$M = \begin{bmatrix} S1 * S7 + S2 * S8 & S3 * S7 + S4 * S8 & S5 * S7 + S6 * S8 \\ S1 * S9 + S2 * S10 & S3 * S9 + S4 * S10 & S5 * S9 + S6 * S10 \\ S1 * S11 + S2 * S12 & S3 * S11 + S4 * S12 & S5 * S11 + S6 * S12 \\ S1 * S13 + S2 * S14 & S3 * S13 + S4 * S14 & S5 * S13 + S6 * S14 \end{bmatrix} = \begin{bmatrix} SaA & SaB & SaC \\ SbA & SbB & SbC \\ ScA & ScB & ScC \\ SnA & SnB & SnC \end{bmatrix} \quad (9)$$

In Figure 1 voltages are:  $V_{out} = \begin{pmatrix} V_a \\ V_b \\ V_c \\ V_n \end{pmatrix}$  and  $V_{in} = \begin{pmatrix} V_A \\ V_B \\ V_C \end{pmatrix}$ .

The mathematical modeling is summarized in Figure 2.

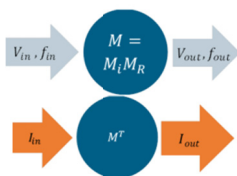


Fig. 2. Mathematical modeling of matrix converter

### III. INDIRECT SPACE VECTOR MODULATION

Indirect space vector modulation can be implemented by splitting the modulation into two stages, the first is called rectifying stage and the second is called inversion stage, to achieve decoupling between the input current control and the output voltage control as per (5) and (9) and based on the assumption of virtual DC link as shown in Figure 1.

#### A. Rectifying Stage

The main function of the rectifying stage is to achieve a control on the displacement angle of the input current and to control the amplitude of the virtual DC link voltage. In the rectifying stage, only two switches must be closed at a time,

just one upper switch and one lower switch can be closed simultaneously to avoid short circuit. The rectifier switches are numbered from one to six as shown in Figure 1. Nine switching combinations are only allowed to guarantee that no short circuit will occur as shown in Figure 3.

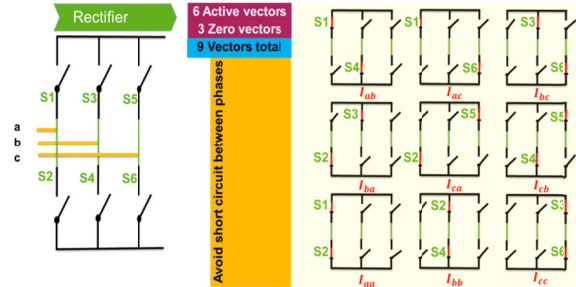


Fig. 3. Nine switching combinations for the rectifying stage

#### B. Rectifier Space Vector Modulation

SVM for the rectifying stage works by transforming input abc to  $\alpha\beta$  coordination and calculating the reference vector angle by which we can define the working sector. For matrix converter modulation requirement, it has been approved by simulation that switching one vector per sector is sufficient and there is no need to synthesize two vectors per sector as commonly happens with conventional rectifier SVM modulations as shown in Figure 4.

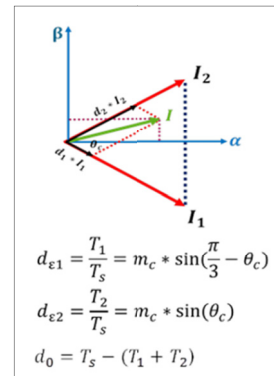


Fig. 4. Synthesis of reference current

In Figure 4,  $\theta_c$  is the angle of the reference current within the actual hexagon sector,  $m_c$  the current modulation index  $= I_{ref} / I_{DC}$ ,  $0 < m_c < 1$ . For matrix converter,  $m_c = 1$  and there is no need to synthesize the reference vector as just one vector will be switched during every sector duration as shown in Figure 5. Modulation process happens by assigning one active vector during the time interval of every sector. Vector selections have been translated into a train of pulses carrying the number of the current sector, numbers are represented in the range of one to six. To achieve the second target of rectifying stage and one of the most interesting features of matrix converter is to have unity power factor at the input side. The displacement angle between input current and voltage shall be zero. To implement this, the reference signal given to the

modulation process has been taken from input phase voltage instead of the input phase current.

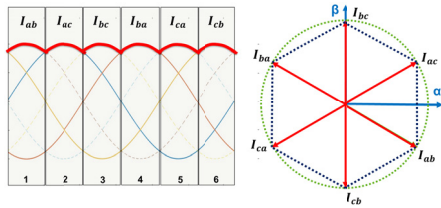


Fig. 5. Rectifying stage SVM vectors selection

III. INVERSION STAGE

Inversion stage is concerned with inverter side SVM modulation, and as this paper discusses four-leg matrix converter, we will address the 3D SVM as a modulation approach for the four-leg matrix converter. The primary function of inversion stage is to provide a control over the output voltage under balanced and unbalanced loads. The added fourth leg is responsible for providing a current path for the zero-sequence component during unbalance. The balanced three-phase system follows (10).

$$X_a + X_b + X_c = 0 \tag{10}$$

And the transformation from abc to  $\alpha\beta$  coordination is applied as it has happened with the rectifier stage. For an unbalanced system (10) is no longer valid and (11) is now applied. Due to the unbalancing of the system, there will be neutral current passing through the system and it is the basic role of 3D SVM to provide accurate switching pulses to all legs.

$$X_a + X_b + X_c \neq 0 \tag{11}$$

Transformation to stationary frame happens into  $\alpha\beta\gamma$  coordination due to the zero-sequence component. In the inversion stage, switches on the same leg can't be turned on at the same time in order to avoid short circuit. For the four-leg inverter with eight switches, the possible switching combinations are sixteen. Switching combinations represented by p or n for each leg, where p indicates the upper switch is turned on (positive) and n indicates the lower switch is on (negative). If the sixteen-vectors are represented into  $\alpha\beta\gamma$  coordination, the result is a 3D hexagon and sectors of conventional SVM are turned into prisms. The 3D hexagon can be divided into six prisms (Figures 6-7). The prisms are an analog to sectors representation on conventional 2D SVM. Prism number may be identified by defining the reference vector angle on  $\alpha\beta\gamma$  coordination.

A. Prism Identification

If

- 0< $\theta$ <60 then P=1
- 60< $\theta$ <120 then P=2
- 120< $\theta$ <180 then P=3
- 180< $\theta$ <240 then P=4

- 240< $\theta$ <300 then P=5
- 300< $\theta$ <360 then P=6, where  $\theta = \tan^{-1} \frac{V_\beta}{V_\alpha}$

Vectors are distributed into each prism as shown in Figure 8. Each prism contains four active vectors.

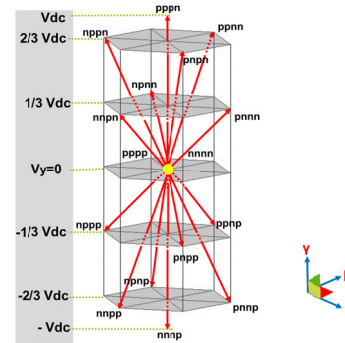


Fig. 6. 3D representation of switching vectors in  $\alpha\beta\gamma$  coordination

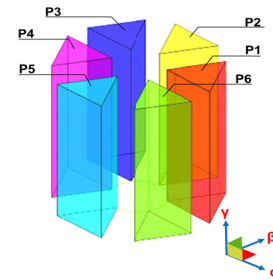


Fig. 7. Prisms identification for 3D SVM

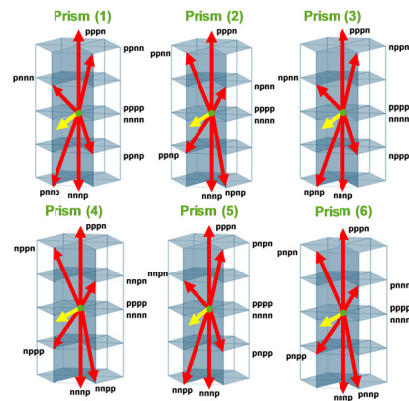


Fig. 8. Vector distribution into each prism

B. Switching Vector Selection

As the reference vector location is defined by prism number and tetrahedron number, selection of switching vectors is implemented by choosing the nearest reference vectors located beside each tetrahedron[8, 9]. Each tetrahedron consists of three switching vectors, to calculate the duty cycle for each switching vector the reference required voltage is transformed

first to  $\alpha\beta\gamma$  coordination and then is divided by the available switching vectors [9] as per (12).

$$\begin{pmatrix} V_{\alpha-ref} \\ V_{\beta-ref} \\ V_{\delta-ref} \end{pmatrix} = [d_1 \quad d_2 \quad d_3] \begin{pmatrix} V_1 \\ V_2 \\ V_3 \end{pmatrix} \quad (12)$$

The duty cycles can be further calculated as shown in (13).

$$\begin{pmatrix} d_1 \\ d_2 \\ d_3 \end{pmatrix} = \frac{1}{V_g} * S * \begin{pmatrix} V_{\alpha-ref} \\ V_{\beta-ref} \\ V_{\delta-ref} \end{pmatrix} \quad (13)$$

$$d_z = 1 - (d_1 + d_2 + d_3) \quad (14)$$

where  $S$  is the duty cycle matrix [8-10],  $(V_{\alpha-ref} \ V_{\beta-ref} \ V_{\delta-ref})^T$  is the reference vector,  $(V_1 \ V_2 \ V_3)^T$  is the current switching vector, and  $d$  represents the duty cycle for each switching vector.  $S$  matrix is dependent on the selected switching vectors, so it has varying values depending on each selected prism and tetrahedron.  $S$  matrix calculations have been done for each possible coincidence between prisms and tetrahedrons. The 3D SVM code checks the prism and tetrahedron number to extract the current values of  $S$ .

#### IV. MATRIX CONVERTER

The rectifying stage is dedicated to generating a series of numbers from 1 to 6, these numbers representing the current active rectifier switches and would be represented on  $M_R$  (rectifier matrix). At the same time the inversion stage is in charge of generating another series of numbers from 1 to 16, representing the current active inverter switches that would be represented on  $M_i$  (inverter matrix) as well. Multiplying the two matrices as in (5) allows us to find all possible switches for matrix converter. The procedure is shown in Figure 9.

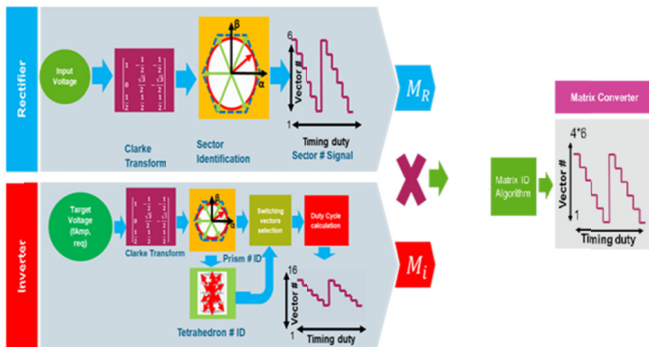


Fig. 9. Matrix converter code generation from  $M_i$  and  $M_R$

#### V. SIMULINK SIMULATION

A Simulink simulation was successfully developed to validate the effectiveness of matrix converter operation under varying types of loads. The proposed indirect 3D SVM was successfully validated as well. Simulation worked under various scenarios such as balanced and unbalanced linear load. The input and output waveforms ensured proper converter operation. The simulation was carried out using the parameters shown in Table I. The simulation results are shown in Figures 10-26.

TABLE I. SYSTEM PARAMETERS

Source system	440V-60Hz
Load system	115V-400Hz
Switching frequency	12800Hz
Input filter (LC)	56Ω/0.8mH/10uF
Output filter (LC)	180uH+70uH/100uF
Repetitive Controller Q(z)	$\frac{z^2 + 2z + 1}{z^2 - 1.723776z + 0.75754}$
Tracking controller	$\frac{z^2 - 1.663z + 0.9914}{z^2 - 1.868z + 0.8735}$
Unbalanced load	5Ω+5.5mH, 10Ω+6.2mH, 20Ω+7.5mH
Balanced load	5Ω +5.5 mH
Nonlinear load	3phase diode bridge +50Ω

#### A. Non-Linear Load

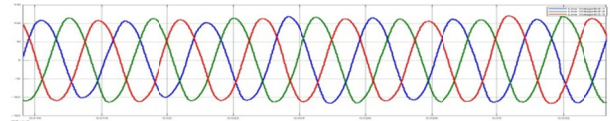
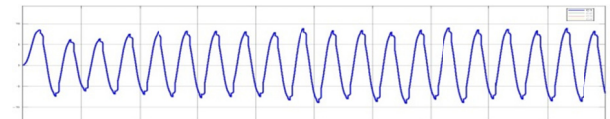
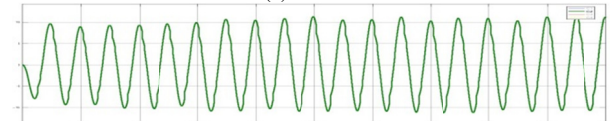


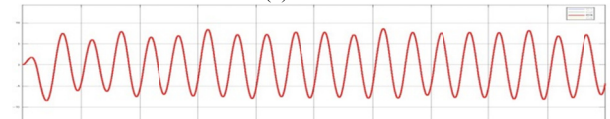
Fig. 10. Output voltage



(a) Phase A



(b) Phase B



(c) Phase C



(d) Neutral

Fig. 11. Output current

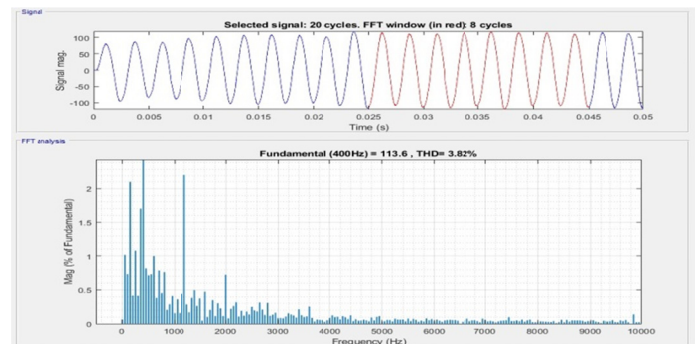


Fig. 12. FFT analysis for output phase voltage (THD=3.3%)

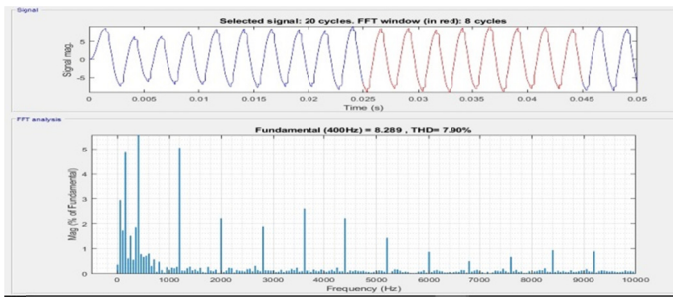


Fig. 13. FFT analysis for output current (THD=1.8%)

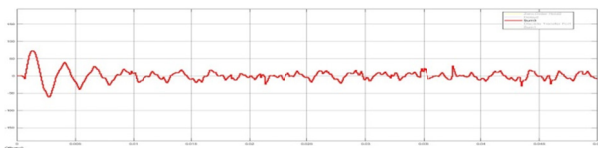


Fig. 14. Error signal

B. Unbalanced Load

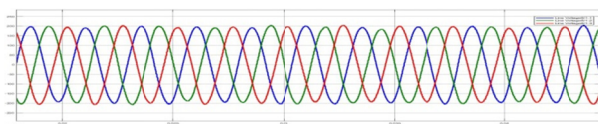
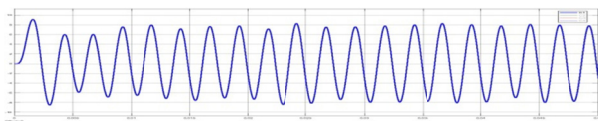
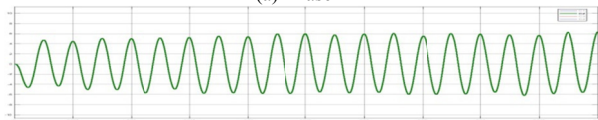


Fig. 15. Output voltage



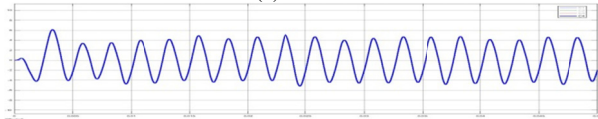
(a) Phase A



(b) Phase B



(c) Phase C



(d) Neutral

Fig. 16. Output Currents



Fig. 17. Input current multiplied by factor 50 and input voltage

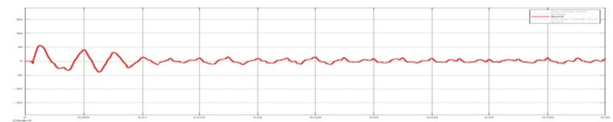


Fig. 18. Error signal

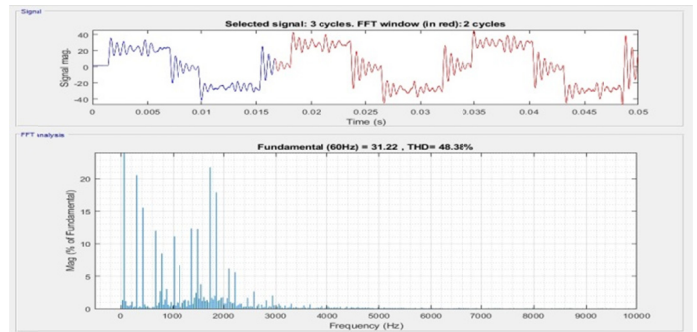


Fig. 19. FFT analysis for input current (THD=48%)

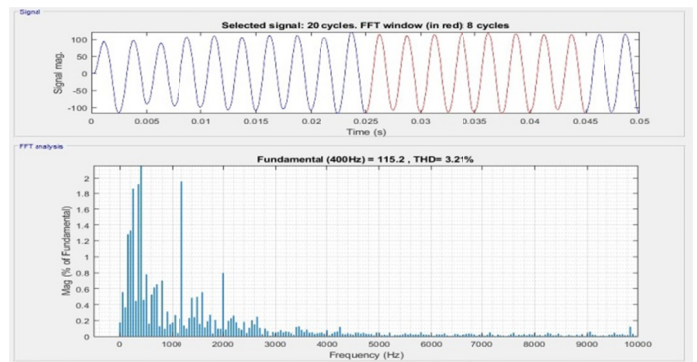


Fig. 20. FFT analysis for output phase voltage (THD=3.3%)

C. Non Linear Load

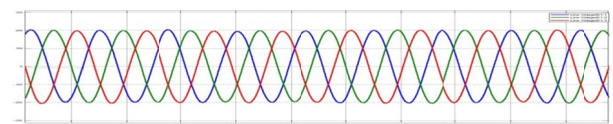


Fig. 21. Output voltage 115V/400H

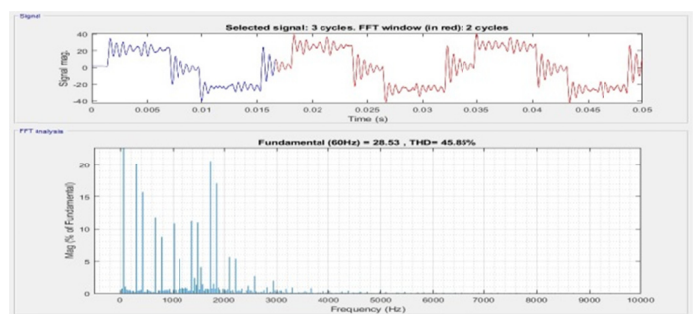


Fig. 22. FFT analysis for input current (THD=48%)

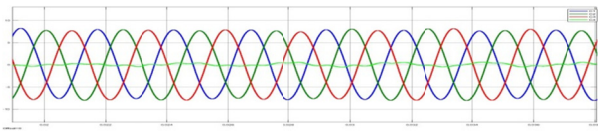


Fig. 23. Output current

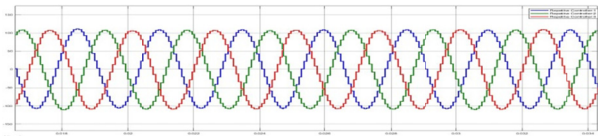


Fig. 24. Repetitive controller output signal

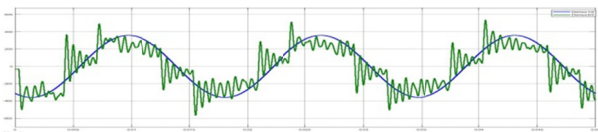


Fig. 25. Input current multiplied by factor 50 and input voltage

## VI. CONCLUSION

This paper introduced the design of 3D SVM indirect modulation for four-leg matrix converter, code validation has been implemented and simulated in Simulink. A repetitive controller was selected to regulate the output voltage due to limited bandwidth for high-frequency applications (115V/400Hz). The simulation results for varying load conditions (balanced, unbalanced, nonlinear) ensured the effectiveness of the proposed modulation technique and repetitive controller showed the ability to regulate the output voltage in an excellent way.

## REFERENCES

- [1] P. Zanchetta, J. C. Clare, P. W. Wheeler, D. Katsis, M. Bland, L. Empringham, "Control Design of a three-phase matrix converter mobile AC power supply using genetic algorithms", IEEE 36th Power Electronics Specialists Conference, Recife, Brazil, pp. 2370-2375, June 16, 2005
- [2] C. Klumpner, F. Blaabjerg, P. Nielsen, "Speeding-up the maturation process of the matrix converter technology", 32nd IEEE Power Electronics Specialist Conference PESC, Vancouver, Canada, Vol. 2, pp. 1083-1088, June 17-21, 2001
- [3] D. Casadei, G. Serra, A. Tani, "The use of matrix converters in direct torque control of induction machines", IEEE Transactions on Industrial Electronics, Vol. 48, No. 6, pp. 1057-1064, 2001
- [4] F. Yue, P. W. Wheeler, N. Mason, L. Empringham, J. C. Clare, "Indirect space vector modulation for a 4-leg matrix converter", IEEE Power Electronics Conference, PESC 2007, Orlando, USA, June 17-21, 2007
- [5] R. Zhang, High performance power converter system for nonlinear and unbalanced load/source, PhD Thesis, Virginia Polytechnic Institute and State University, 1998
- [6] R. Cárdenasa, R. Penab, J. Clare, P. Wheeler, P. Zanchetta, "A repetitive control system for four-leg matrix converters feeding non-linear loads", Electric Power Systems Research, Vol. 104, pp. 18-27, 2013
- [7] T. Friedli, J. W. Kolar, J. Rodriguez, P. W. Wheeler, "Comparative evaluation of three-phase AC-AC matrix converter and voltage DC-link back-to-back converter systems", IEEE Transactions on Industrial Electronics, Vol. 59, No. 12, pp. 4487-4510, 2012
- [8] V. H. Prasad, D. Boroyevich, R. Zhang, "Analysis and comparison of space vector modulation schemes for a four-leg voltage source inverter", 12th Annual Applied Power Electronics Conference and Exposition (APEC), Atlanta, USA, Vol. 2, pp. 864-871, February 27, 1997
- [9] R. Zhang, V. H. Prasad, D. Boroyevich, F. C. Lee, "Three-dimensional space vector modulation for four-leg voltage- source converters", IEEE Transactions on Power Electronics, Vol. 17, No. 3, pp. 314-326, 2002
- [10] R. Zhang, D. Boroyevich, V. H. Prasad, H. C. Mao, F. C. Lee, S. Dubovsky, "A three-phase inverter with a neutral leg with space vector modulation", 12th Annual Applied Power Electronics Conference and Exposition, Atlanta, USA, Vol. 2, pp. 857-863, February 27, 1997
- [11] L. Empringham, P. W. Wheeler, J. C. Clare, "Intelligent commutation of matrix converter bi-directional switch cells using novel gate drive techniques", 29th Annual IEEE Power Electronics Specialists Conference, Vol. 1, pp. 707-713, May 22, 1998
- [12] J. Mahlein, J. Igney, J. Weigold, M. Braun, O. Simon, "Matrix converter commutation strategies with and without explicit input voltage sign measurement", IEEE Transactions on Industrial Electronics, Vol. 49, No. 2, pp. 407-414, 2002
- [13] W. Hofmann, M. Ziegler, "Multi-step commutation and control policies for matrix converters", Journal of Power Electronics, Vol. 3, No. 1, pp. 24-32, 2003
- [14] B. H. Kwon, B. D. Min, J. H. Kim, "Novel commutation technique of AC-AC converters", IEE Proceedings-Electric Power Applications, Vol. 145, No. 4, pp. 295-300, 1998
- [15] P. W. Wheeler, J. Rodriguez, J. C. Clare, L. Empringham, A. Weinstein, "Matrix converters: a technology review", IEEE Transactions on Industrial Electronics, Vol. 49, No. 2, pp. 276-288, 2002
- [16] E. Ormaetxea, J. Andreu, I. Kortabarria, U. Bidarte, I. Martinez de Alegria, E. Ibarra, E. Olaguena, "Matrix converter protection and computational capabilities based on a system on chip design with an FPGA", IEEE Transactions on Power Electronics, Vol. 26, No. 1, pp. 272-287, 2011
- [17] D. Casadei, G. Serra, A. Tani, L. Zarri, "A review on matrix converters", Przegląd Elektrotechniczny, Vol. 82, No. 2, pp. 15-25, 2006
- [18] L. Empringham, P. W. Wheeler, J. C. Clare, "Bi-directional switch current commutation for matrix converter applications", 8th International Power Electronics & Motion Control Conference, Prague, Czech Republic, pp. 42-47, September 8-10, 1998
- [19] M. Ziegler, W. Hofmann, "New one-step commutation strategies in matrix converters", 4th IEEE International Conference on Power Electronics and Drive Systems, Bali, Indonesia, Vol. 2, pp. 560-564, 2001
- [20] M. Ziegler, W. Hofmann, "A new two steps commutation policy for low cost matrix converters", 41st PCIM/Power Quality Conference, Nürnberg, Germany, pp. 445-450, 2000
- [21] M. Ziegler, W. Hofmann, "Semi natural two steps commutation strategy for matrix converters", 29th Annual IEEE Power Electronics Specialists Conference (PESC'98), Fukuoka, Japan, pp. 727-731, May 22, 1998
- [22] D. Casadei, A. Trentin, M. Matteini, M. Calvini, "Matrix converter commutation strategy using both output current and input voltage sign measurement", European Conference on Power Electronics and Applications (EPE'03), Toulouse, France, pp. P1-P10, 2003
- [23] L. Empringham L, L. de Lillo, S. Khwan-On, C. Brunson, P. W. Wheeler, J. C. Clare, "Enabling technologies for matrix converters in aerospace applications", International Conference Workshop Compatibility and Power Electronics (CPE'2011), Tallinn, Estonia, pp. 451-456, 2011